Direct observation of structure effect on ferromagnetism in $Zn_{1-x}Co_xO$ nanowires

W. B. Jian*
Department of Electrophysics, National Chiao Tung University, Hsinchu 300, Taiwan

Z. Y. Wu, R. T. Huang, F. R. Chen, and J. J. Kai
Department of Engineering and System Science, National Tsing Hua University, Hsinchu 300, Taiwan

C. Y. Wu
Opto-Electronics and Systems Laboratories, Industrial Technology Research Institute, Hsinchu 310, Taiwan

S. J. Chiang and M. D. Lan
Department of Physics, National Chung Hsing University, Taichung 402, Taiwan

J. J. Lin†
Institute of Physics and Department of Electrophysics, National Chiao Tung University, Hsinchu 300, Taiwan
(Received 20 July 2005; revised manuscript received 14 April 2006; published 21 June 2006)

Diameter-controllable single-crystalline ZnO nanowires (NWs), with the [0001] growth direction in the plane, have been fabricated by using thermal evaporation method. The as-grown NWs with diameters of ~40 nm were implanted with various amounts of Co ions. These $Zn_{1-x}Co_xO$ ($x \leqslant 0.11$) NWs possessed a high density of bombardment-induced orientation variations and stacking faults, and exhibited paramagnetic behavior. After thermal annealing, the structural defects largely disappeared and noticeable hysteresis in the magnetization loops were observed, indicating the presence of apparent ferromagnetic ordering in the NWs. This result provides important insight into the role played by defects in relation to the occurrence of ferromagnetism in diluted magnetic semiconductor NWs.

DOI: 10.1103/PhysRevB.73.233308 PACS number(s): 75.75.+a, 75.50.Pp, 81.07.−b

I. INTRODUCTION

Not only a high Curie temperature T_C, but also the mechanism of ferromagnetism in diluted magnetic semiconductors (DMS) has recently drawn intense attention. Theoretically, it has been proposed that the ferromagnetism in III-V based DMS materials, (In,Mn)As and (Ga,Mn)As, is mediated by the mobile holes originating from the magnetic Mn dopants.[1–3] The ferromagnetic *p*-type (Ga,Mn)As with a high carrier density of 10^{18}–10^{20} cm^{-3} could possess a T_C as high as 110 K.[3] It has also been argued that the T_C of the *p*-type Mn-doped ZnO semiconductor, with a carrier concentration of 3.5×10^{20} cm^{-3}, could be as high as the room temperature. Recently, these theoretical proposals have stimulated extensive efforts to search for high-T_C DMS ferromagnets.[4–6] In particular, *ab initio* and first-principles calculations,[7–11] and some recent experiments[12] showed a ferromagnetic phase in the *n*-type ZnO doped with Co. Experimentally, significant discrepancies have been reported among different groups and between the measurements and the theoretical calculations. For example, Ueda *et al.*[4] reported room-temperature ferromagnetism in pulse laser deposited $Zn_{1-x}Co_xO$ thin films. Other groups[5,13] reported ferromagnetism above room temperature even in nanophased structures.[14,15] On the contrary, Risbud *et al.*[16] and Lawes *et al.*[17] found no ferromagnetism in Co substituted polycrystalline ZnO. Thus far, very few experiments have been performed on $Zn_{1-x}Co_xO$ nanowires (NWs) to see the direct correspondence between structure and ferromagnetism.

ZnO is an oxide semiconductor with a room temperature energy gap of 3.37 eV. In contrast to the other II-VI compound semiconductors, ZnO can be heavily doped to form a transparent conductor.[18] Since nanostructures are potentially ideal functional components for nanoelectronic and optoelectronic devices, the study of ZnO NWs is of high interest. Realization of spintronic devices from the bottom up might be feasible by adopting the DMS Co-doped ZnO NWs.[19,20]

In addition to the amount of carrier concentration, it is theoretically accepted that crystalline quality and structural defects should play an important role in determining the occurrence and stability of ferromagnetism.[16,21,22] However, there has been no *direct* experimental observation to discern this conjecture. In this work, we use as-implanted and annealed $Zn_{1-x}Co_xO$ NWs (Ref. 23) to explore the detrimental effects of defects on ferromagnetism. Compared with the bulk and thin film samples, NW samples have the advantage that no additional mechanical treatment of the specimens (which might introduce unwanted changes in the crystal structure) was needed for the transmission electron microcopy (TEM) studies.

II. EXPERIMENT

ZnO powder was placed in a crucible situated at the center of a quartz tube in a furnace heated to 950 °C. A glass substrate at a temperature of 500 °C with gold nanoparticles (~40 nm in diameter) as catalysts predeposited on it was located at the downstream end of the quartz tube. The chamber was maintained at 200 Pa with a constant flow of argon. After 8 h, ZnO NWs with an average diameter of 40 nm formed. The as-grown ZnO NWs were implanted by Co ions

with doses of $(1-6)\times10^{16}$ cm^{-2}. The implantation was performed at room temperature with an accelerating energy of 40 keV by using a tandem accelerator (9SDH-2). The beam current was kept at 150 nA/cm^2 to avoid beam heating. Annealing of the as-implanted ZnO NWs was then performed at 600 °C for 12 h either under an *argon* flow of 150 sccm at 1 atm or in a *vacuum* of 5×10^{-5} torr. This annealing temperature was chosen because it would not cause aggregation and clustering of the implanted ions, as was previously established[24] for ZnO and was confirmed by our high-resolution transmission electron microscopy (HRTEM) studies. Annealing in argon would not only prevent oxidation of the samples and substrates but also improve the lattice order. On the other hand, annealing in vacuum would produce oxygen deficiencies and increase *n*-type carriers.[22,25,26] Both the as-implanted and annealed ZnO NWs were characterized by using a field-emission scanning electron microscope (JEOL JSM-6330F) and HRTEM (JEOL JEM-2010F). Magnetic properties of the NWs were studied by using a Quantum Design superconducting quantum interference device (SQUID) magnetometer. All the magnetizations as a function of applied field were taken at 2 K, unless otherwise stated. It should be noted that the magnetic responses were large such that no corrections for the sample holder and the substrate were needed. For instance, the magnetizations at 2 K and in a field of 1000 Oe were 1.4×10^{-5} emu for the substrate alone and 2.8×10^{-4} emu for the substrate with $Zn_{1-x}Co_xO$ NWs.

III. RESULTS AND DISCUSSION

Most of our ZnO NWs with a length of several microns lay on the substrate with [0001] growth direction in the plane and form a NW film of about 3.7 μm thick on the substrate. High-energy Co ions were bombarded on one side to produce DMS NWs. Computer simulation SRIM code[27] enabled us to estimate the distribution of Co ions in the ZnO NWs. When implanting in bulk, the Co-ion density distribution as a function of penetration depth showed a range of 40 nm, close to the diameter (~40 nm) of our NWs. Figure 1(a) shows a scanning electron microscopy (SEM) image of representative as-implanted NWs. We found that the morphology and dimension of the ZnO NWs did not change appreciably after Co implantation except for a slight bending of the NWs. To ensure that the implanted Co ions distributed uniformly, rather than aggregated, in the NWs, we performed energy dispersive x-ray spectroscopy (EDX) and bright field TEM studies. The right image of the inset in Fig. 1(b) shows an EDX compositional map revealing Co distribution in a NW, while the left image of the inset in Fig. 1(b) shows a bright field TEM image for the same NW. In addition, maps of the electron energy loss spectroscopy (EELS) have been carried out to exclude any formation of Co clusters larger than 1.8 nm. These results strongly indicate the uniformity of Co ions in the NWs. The Co atom implantation generated a thin layer of $Zn_{1-x}Co_xO$ NWs on the top of the as-grown ZnO NW film on the substrate. The thickness of this DMS NW layer can be evaluated as follows. We know that the bombardment of 1×10^{16} cm^{-2} Co ions produced the as-implanted $Zn_{0.98}Co_{0.02}O$ NWs from EDX analysis. Assuming a uniform layer of the $Zn_{0.98}Co_{0.02}O$ material, we estimated the thickness of this layer to be about 120 nm which was used for evaluation of the sample volume and magnetization.

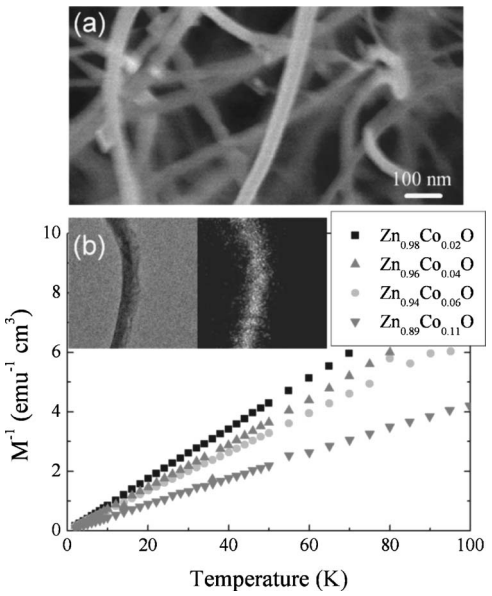

FIG. 1. (a) Typical SEM image of the as-implanted $Zn_{0.94}Co_{0.06}O$ NWs. (b) The inverse magnetizations of as-implanted $Zn_{1-x}Co_xO$ NWs taken at a field of 1000 Oe. Inset: A bright field TEM image of a NW (left) together with its corresponding EDX mapping image (right).

The main panel of Fig. 1(b) shows a plot of the inverse magnetizations of our $Zn_{1-x}Co_xO$ NWs with several concentrations x. The inverse magnetization for every NW varies linearly with temperature and diminishes at zero temperature, indicating that these as-implanted NWs display *paramagnetism* closely obeying the Curie law. As x increases, the paramagnetic behavior becomes more pronounced in accordance with the Co concentrations determined from the EDX spectra. The effective moment for the implanted Co ions in the DMS NWs was extracted and found to be 1–2 times of the ideal value ($4.8\mu_B$) for Co^{2+}.[28] This overestimation arose from the uncertainties in the evaluation of the sample volume.

The as-implanted NWs exhibit paramagnetism, barely revealing any signature of ferromagnetic ordering [squares in Fig. 3(a)]. High densities of structural defects are produced during the high-energy Co-ion bombardment. The structure of the NWs was therefore investigated in detail. The HRTEM image shown in Fig. 2 displays one type of structural defects, i.e., stacking faults, as indicated by the many small triangles. Another type of structural defects is orientation variations, a typical diffraction pattern of which is shown for the as-implanted $Zn_{0.89}Co_{0.11}O$ NWs in the inset of Fig. 2. It is seen that the lattice planes along the [0001] direction are fairly ordered while there is orientation variation between the $(11\bar{2}0)$ lattice planes.

To see the detrimental effects of defects on ferromagnetism in DMS, and particularly in Co-doped ZnO NWs, we have carried out systematic thermal annealing and magnetization measurements on our NWs. Figure 3(a) shows the

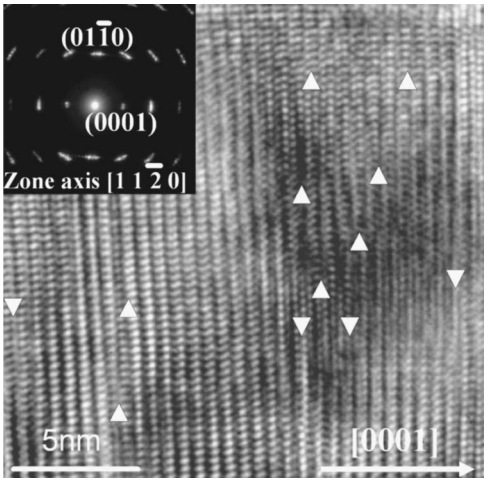

FIG. 2. HRTEM image of the as-implanted $Zn_{0.89}Co_{0.11}O$ NWs with white triangles indicating stacking faults. Inset: A typical diffraction pattern revealing a rotation of reciprocal lattice points.

field-dependent magnetizations for the representative $Zn_{0.89}Co_{0.11}O$ NWs. Similar magnetization behavior has also been observed in other NWs with different Co concentrations. Figure 3(a) illustrates that the argon-annealed NWs (circles) displayed a noticeable hysteresis loop, indicating the occurrence of ferromagnetism.

It is important to clarify whether the enhanced hysteresis loop observed in the argon-annealed NWs might be due to any aggregation of Co ions as a result of implantation. To disprove this conjecture, we have studied the magnetizations of several $Zn_{1-x}Co_xO$ NWs annealed under a high vacuum. The triangles in Fig. 3(a) reveal the magnetization of the vacuum-annealed $Zn_{0.89}Co_{0.11}O$ NWs at 2 K. It is clearly seen that the hysteresis loop becomes enormously enlarged, suggesting strong ferromagnetism. We also found that, as the temperature increases, the hysteresis loop squeezes (not shown), indicating the depression of the ferromagnetic ordering. These results argue against the possibility of aggregated Co ions induced magnetism. If the Co atoms had aggregated in our NWs, their structural configurations should have *barely* changed under our annealing conditions and the magnetizations should be *very similar* for the argon- and vacuum-annealed samples.

Furthermore, we have performed *second* annealing in 1 atm of either oxygen or argon atmosphere on those already vacuum-annealed samples. Noticeably, we found an appreciable shrinkage of the hysteresis loops with attenuated magnetizations for those that underwent second annealing in oxygen, but we found no change in the magnetic properties for those that underwent second annealing in argon. The structure of all the annealed NWs was inspected in detail by using the HRTEM and no perceptible change was spotted. In fact, it is known[25] that preparing $ZnO_{1-\delta}$ thin films under high vacuum could increase the oxygen vacancies and reduce the electrical resistivity. It has also been reported that transition-metal doped ZnO thin films grown in oxygen[29] rarely showed hysteresis loops, while they might display strong ferromagnetism even at room temperatures if grown in vacuum.[30] Thus, we think that the enhanced ferromagnetism found in the vacuum-annealed NWs must be closely

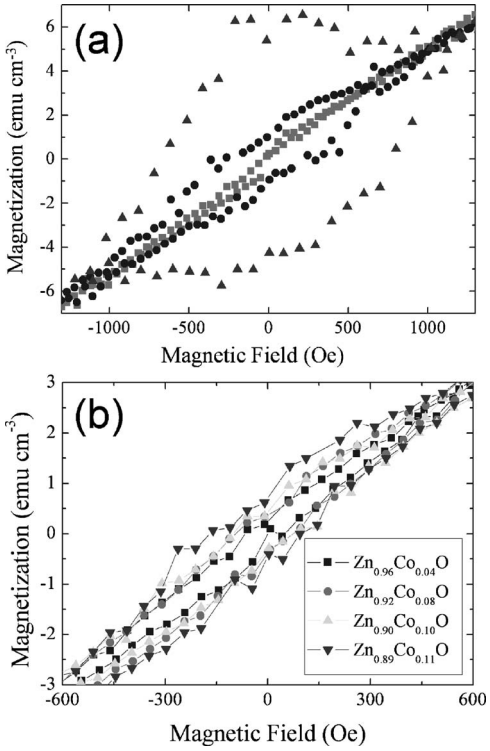

FIG. 3. (a) Magnetization as a function of applied field at 2 K for as-implanted (squares), argon-annealed (circles), and vacuum-annealed (triangles) $Zn_{0.89}Co_{0.11}O$ NWs. The magnetization has been scaled by dividing the number 11 for comparison with (b). (b) Magnetization as a function of applied field at 2 K for argon-annealed $Zn_{1-x}Co_xO$ NWs with different x as indicated. The magnetization for each concentration has been scaled (see text).

connected with not only the improved structure but also likely with an increased number of carriers. The current theoretical concept of the carrier-mediated ferromagnetism in DMS might be relevant to our case.

To further inspect any possible aggregation of Co atoms in our NWs, in addition to the bright field TEM and EDX studies [Fig. 1(b)], we have performed systematic HRTEM and EELS measurements. Any possible aggregated microstructure and aggregated Co elements can be detected by HRTEM and EDX, respectively, and the aggregated Co ions with specified oxidation state can be identified by EELS. Our HRTEM studies indicate no evidence of any Co-atom aggregation down to the scale limit of 0.5 nm, and our EELS analysis points to the valence state of Co ion in the argon-annealed NWs to be close to +2. The valence state of the Co ion in the vacuum-annealed NWs is slightly shifted to a high oxidation state of +2.67, which is definitely not the valence state of Co metal. These results strongly argue against the existence of Co clustering and segregation in our NWs.

Figure 3(b) shows the magnetizations of argon-annealed $Zn_{0.96}Co_{0.04}O$, $Zn_{0.92}Co_{0.08}O$, $Zn_{0.90}Co_{0.10}O$, and $Zn_{0.89}Co_{0.11}O$ NWs divided by factors of 4, 8, 10, and 11, respectively, for comparison. We see that the hysteresis loops become more pronounced with increasing Co concentration, implying the formation of domains as well as the enhanced exchange interactions between Co ions. Meanwhile, the magnetization increases with increasing Co implantation,

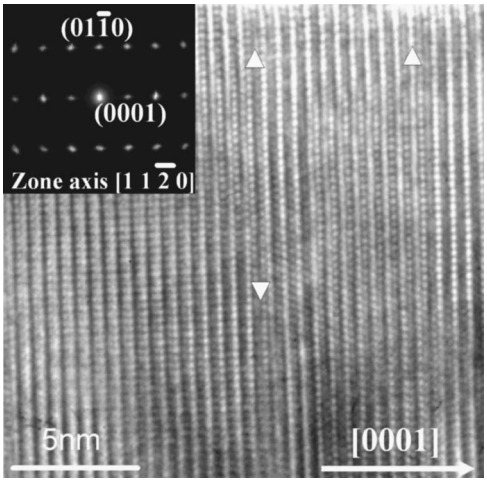

FIG. 4. HRTEM image for argon-annealed $Zn_{0.89}Co_{0.11}O$ NWs with white triangles indicating stacking faults. Inset: A typical diffraction pattern showing regular reciprocal lattice points.

confirming the occurrence of ferromagnetic, but not previously reported antiferromagnetic,[16] ordering among Co ions. Moreover, this result implies the absence of a second phase of CoO in our NWs, since CoO is antiferromagnetic with a Neel temperature of 291 K.

The structure of our annealed $Zn_{1-x}Co_xO$ NWs was then inspected by HRTEM. The diffraction pattern in the inset of Fig. 4 clearly reveals disappearance of orientation variations. The lattice points along the $[01\bar{1}0]$ direction are now well ordered. In addition, the HRTEM image of the argon-annealed $Zn_{0.89}Co_{0.11}O$ (the main panel of Fig. 4) shows a significant reduction in the density of stacking faults. A very similar result has also been observed in those high-vacuum annealed NWs. Therefore, it is clear that the improved lattice order must lead to the enhanced ferromagnetism found in the annealed $Zn_{1-x}Co_xO$ NWs. In other words, the ferromagnetism was deprived due to the presence of a high density of structural defects before annealing. In short, our observations clearly indicate that structural defects are detrimental to the occurrence of ferromagnetic ordering in DMS NWs. Any theoretical model attempting to explain the mechanism of ferromagnetism in $Zn_{1-x}Co_xO$ must take this result into account.[1,2]

IV. CONCLUSION

In this work, 40-nm diameter $Zn_{1-x}Co_xO$ NWs were synthesized by thermal evaporation, followed by high-energy Co-ion implantation. The implanted Co ions were uniformly distributed in the NWs but the implantation produced many orientation variations and stacking faults in the NWs. After annealing, the crystalline lattice order was essentially recovered. The magnetizations then indicated apparent ferromagnetic behavior. This work provides strong evidence for the close connection between the structural order and the occurrence of ferromagnetism in DMS $Zn_{1-x}Co_xO$ NWs.

ACKNOWLEDGMENTS

This work was supported by the Taiwan National Science Council under Grants No. NSC 93-2112-M-009-038, No. NSC 93-2120-M-009-009, and No. NSC 94-2120-M-009-010, and by the MAU ATU Program.

*Electronic address: wbjian@mail.nctu.edu.tw
†Electronic address: jjlin@mail.nctu.edu.tw

[1] T. Dietl *et al.*, Science **287**, 1019 (2000).
[2] H. Akai, Phys. Rev. Lett. **81**, 3002 (1998).
[3] F. Matsukura *et al.*, Phys. Rev. B **57**, R2037 (1998).
[4] K. Ueda *et al.*, Appl. Phys. Lett. **79**, 988 (2001).
[5] H.-J. Lee *et al.*, Appl. Phys. Lett. **81**, 4020 (2002).
[6] D. P. Norton *et al.*, Appl. Phys. Lett. **82**, 239 (2003).
[7] K. Sato and H. Katayama-Yoshida, Jpn. J. Appl. Phys., Part 2 **40**, L334 (2001).
[8] M. H. F. Sluiter *et al.*, Phys. Rev. Lett. **94**, 187204 (2005).
[9] C. H. Park and D. J. Chadi, Phys. Rev. Lett. **94**, 127204 (2005).
[10] Q. Wang *et al.*, Phys. Rev. B **70**, 052408 (2004).
[11] N. A. Spaldin, Phys. Rev. B **69**, 125201 (2004).
[12] K. R. Kittilstved *et al.*, Nat. Mater. **5**, 291 (2006).
[13] S. Ramachandran *et al.*, Appl. Phys. Lett. **84**, 5225 (2004).
[14] J.-J. Wu *et al.*, Appl. Phys. Lett. **85**, 1027 (2004).
[15] K. Ip *et al.*, J. Vac. Sci. Technol. B **21**, 1476 (2003).s
[16] A. S. Risbud *et al.*, Phys. Rev. B **68**, 205202 (2003).
[17] G. Lawes *et al.*, Phys. Rev. B **71**, 045201 (2005).
[18] K. Ip, *et al.*, Appl. Phys. Lett. **84**, 544 (2004).
[19] Y. Ohno *et al.*, Nature (London) **402**, 790 (1999).
[20] S. A. Wolf *et al.*, Science **294**, 1488 (2001).
[21] Y. W. Heo *et al.*, Appl. Phys. Lett. **84**, 2292 (2004).
[22] Y. M. Cho *et al.*, Appl. Phys. Lett. **80**, 3358 (2002).
[23] F. Tuomisto *et al.*, Phys. Rev. Lett. **91**, 205502 (2003).
[24] E. Sonder *et al.*, J. Appl. Phys. **64**, 1140 (1988).
[25] A. Tiwari *et al.*, J. Appl. Phys. **96**, 3827 (2004).
[26] C. Ronning *et al.*, Appl. Phys. Lett. **84**, 783 (2004).
[27] J. F. Ziegler and J. P. Biersak, http://www.srim. org
[28] C. Kittel, *Introduction to Solid State Physics* (Wiley, New York, 1996).
[29] W. Prellier *et al.*, Appl. Phys. Lett. **82**, 3490 (2003).
[30] K. Rode *et al.*, J. Appl. Phys. **93**, 7676 (2003).